Author's personal copy

Journal of Marine Systems 82 (2010) 47–60

Contents lists available at ScienceDirect

Journal of Marine Systems

journal homepage: www.elsevier.com/locate/jmarsys

Satellite monitoring of climatic factors regulating phytoplankton variability in the Arabian (Persian) Gulf

Nikolay P. Nezlin [a,*], Igor G. Polikarpov [b,c], Faiza Y. Al-Yamani [b], D.V. Subba Rao [d], Alexander M. Ignatov [e]

[a] Southern California Coastal Waters Research Project, CA, USA
[b] Kuwait Institute for Scientific Research, Kuwait
[c] Institute of Biology of the Southern Seas, Sevastopol, Ukraine
[d] Bedford Institute of Oceanography, Dartmouth, N.S., Canada
[e] NOAA/NESDIS/Office of Research and Applications, MD, USA

ARTICLE INFO

Article history:
Received 15 April 2009
Received in revised form 3 March 2010
Accepted 8 March 2010
Available online 20 March 2010

Keywords:
Oceanography
Remote sensing
Chlorophyll
Seasonal variations
Aerosols
Aeolian dust
Arabian (Persian) Gulf
23°–31°N
47°–56°E

ABSTRACT

Possible factors regulating phytoplankton variability in the Arabian (Persian) Gulf were analyzed on the basis of satellite observations and meteorological data (1997–2009), including remotely-sensed chlorophyll *a* concentration (CHL), sea surface temperature, wind, solar radiation, precipitation, and aerosols. Shallow waters of northwestern Gulf influenced by Shatt Al-Arab River discharge were more productive than open Gulf waters, although seasonal CHL patterns in this and other shallow regions looked unrealistic likely because the CHL signal was obscured by bottom reflection. Therefore our further analyses focused on the open Gulf waters, which show a subtropical seasonal CHL cycle with maximum in winter and minimum in spring–summer. This cycle, however, was decoupled from the seasonal extremes of wind mixing. Interannual variations of CHL in the open Gulf regions were correlated with precipitation and aerosol data rather than with wind and sea surface temperature, consistent with the hypothesis of atmospheric deposition as a factor regulating phytoplankton growth. The effect of dust fertilization was likely observed in 2000 and 2008, when low precipitation and aerosol properties indicating elevated level of aeolian dust transport were followed by phytoplankton blooms.

© 2010 Elsevier B.V. All rights reserved.

1. Introduction

This study is focused on the analysis of seasonal and interannual variabilities of remotely-sensed chlorophyll *a* concentration (CHL) in the Arabian (Persian) Gulf (hereafter the Gulf). CHL measured by Sea-viewing Wide Field-of-view Sensor (SeaWiFS) and MODerate Resolution Imaging Spectroradiometer (MODIS) satellite instruments was analyzed as a proxy of phytoplankton biomass in conjunction with the environmental factors potentially related to phytoplankton growth and distribution: sea surface temperature (SST), wind, photosynthetically available radiation (PAR), precipitation, and aerosol properties related to aeolian dust transport.

Due to specific features of the region, the mechanisms regulating the variability of remotely-sensed CHL in the Gulf may be significantly different from the processes typical to most parts of the ocean. Among the factors analyzed in this study, wind mixing is an important factor regulating vertical stratification of water column and phytoplankton biomass at seasonal time scale (Longhurst, 1995). In deep ocean regions, phytoplankton growth is stimulated, on the one hand, by stratification retaining phytoplankton cells in the upper euphotic layer and, on the other hand, by vertical mixing and upwelling transporting nutrient-rich deep water to the surface. In shallow parts of the Gulf, euphotic layer often extends to the bottom (Subba Rao and Al-Yamani, 1999a) and is well mixed. In the waters with thermal stratification, low SST indicates vertical mixing or upwelling. It is not clear how this relationship works in the open waters of the Gulf, which are generally characterized by haline stratification. Positive correlation between PAR and phytoplankton biomass is expected in the regions where phytoplankton growth is light-limited. Dust deposition enriches ocean waters with micronutrients (e.g., iron), stimulating phytoplankton growth in iron-limited zones (Duce and Tindale, 1991; Martin et al., 1994; deBaar et al., 1995; Jickells et al., 2005; Mahowald et al., 2005), although sometimes the effect of desert dust deposition can be negative (e.g., Mallet et al., 2009; Paytan et al., 2009). It is still unknown how these mechanisms (including iron limitation) work under specific meteorological and oceanographic conditions of the Gulf.

In the absence of direct observations of dust deposition, we analyze aerosol properties measured by SeaWiFS and MODIS-Terra satellite sensors as indicators of aeolian dust concentration. Aerosol optical depth (or optical thickness) is the degree to which aerosols prevent the transmission of light; it characterizes total concentration

* Corresponding author. 3535 Harbor Blvd., Suite 110, Costa Mesa, CA 92626, USA. Tel.: +1 714 755 3227; fax: +1 714 755 3299.
E-mail address: nikolayn@sccwrp.org (N.P. Nezlin).

0924-7963/$ – see front matter © 2010 Elsevier B.V. All rights reserved.
doi:10.1016/j.jmarsys.2010.03.003

Author's personal copy

of aerosols in the atmosphere. Ångström exponent characterizes the spectral dependence of the optical depth. It is correlated with the aerosol particle size spectra and is especially sensitive to desert dust concentration in the atmosphere, which is characterized by large particles resulting in low Ångström exponent values (Husar et al., 1997; Dubovik et al., 2002). High aerosol dust loads in the atmosphere are associated with high rates of dust deposition over ocean waters, which was demonstrated by direct measurements ship-board and at coastal sites, including sediment trap estimates and trace metal concentrations in seawater (see Guerzoni et al., 1999 and the references therein). The relationship between dust deposition (assessed on the basis of aerosol properties) and phytoplankton biomass (estimated from remotely-sensed CHL measurements) is a special focus of this study.

2. Study area

The Gulf is a large shallow embayment of the northern Arabian Sea (Fig. 1). Its length is ~990 km, maximal width is 370 km, and total area is 239,000 km^2. The Gulf is quite shallow (the average depth is approximately 36 m) over the entire extent and its entrance (the Strait of Hormuz) has no blocking sill. The bathymetry is basically asymmetric along the main axis with a deeper zone close to Iranian coast (deepest trough by 120 m) and a broad shallow shelf (<10 m) along the southern and western coasts from Kuwait to United Arab Emirates. The shallow depth and very high net evaporation rate (estimated by different authors as 1.44–1.68 m yr^{-1} (Privett, 1959; Johns et al., 2003)), typical of this arid region, result in hypersaline water mass production, especially intensive in the southern shallow coastal waters east of Qatar, where salinity can be >42 psu. Formation of hypersaline water leads to inverse estuarine circulation with the highly saline waters concentrating in the bottom layer, leaving the Gulf through the deep part of the Strait of Hormuz and the Gulf of Oman and spreading at the depth 200–300 m throughout the Arabian Sea (Banse, 1997; Prasad et al., 2001). Evaporated water is replaced by a surface inflow of lower salinity (~36.5 psu) from the Gulf of Oman. This inflow, penetrates into the Gulf and is carried northwards along the Iranian coast, gradually increasing in salinity to more than 40 psu (Reynolds, 1993). The inflow is seasonal, with maximum in late spring (Swift and Bower, 2003), when it spreads as far as the northwestern part of the Gulf.

The main freshwater supply of the Gulf comes from the Tigris, Euphrates and Karun rivers, which all discharge into the Shatt Al-Arab waterway in Kuwaiti and Iraqi coast. The estimates of river discharge volume vary between 36 and 110 km^3 yr^{-1}, i.e., 0.15–0.46 m yr^{-1} averaged over the entire Gulf area (Reynolds, 1993). Maximum freshwater discharge occurs in late spring–early summer. Precipitation over the Gulf area is also very low (0.07–0.1 m yr^{-1}) (e.g., Marcella and Eltahir, 2008); the total freshwater input is less than the evaporation rate by a factor of 5–10. The Shatt Al-Arab discharge is expected to amplify the Saudi–Emirate coastal current (Reynolds, 1993); its influence is especially evident along the southwestern Gulf coast from Iraq to Qatar.

Deep part of the Gulf is characterized by pronounced haline stratification (Brewer and Dyrssen, 1985; Reynolds, 1993; Swift and Bower, 2003). In contrast, water column in the shallow (<10–15 m) northern, western and southern Gulf is well mixed as a result of wind stress and tidal turbulence (John, 1992). Off Kuwait, spring tidal ranges are 2 m in the south and up to 4 m in the north, while off Bahrain the range is 2 m at extreme springs (Sheppard, 1993). At the same time, deep regions are characterized by much shorter flushing time than coastal regions: 1–3 yr in open waters vs. 3.5 yr in northwestern coastal and >5 yr in southern coastal zone (Sadrinasab and Kampf, 2004).

Persistent northwesterly winds produce southeastward coastal currents and resulting upwelling along the northeastern (Iranian) and downwelling along the southwestern (Saudi) coasts (Reynolds, 1993). Winds are most intensive in spring–summer when the intense "Shamal" events propagate from the northwest to the central and southern Gulf. During autumn the winds are weaker and less variable. Intense temperature differences between land and water result in strong breeze winds, which in turn stimulate intensive mixing processes in coastal regions (Elshorbady et al., 2006).

The area around the Gulf is one of the main sources of aeolian dust in the world (Husar et al., 1997) and strong wind events in this region are often associated with dust storms. For example, in Kuwait region

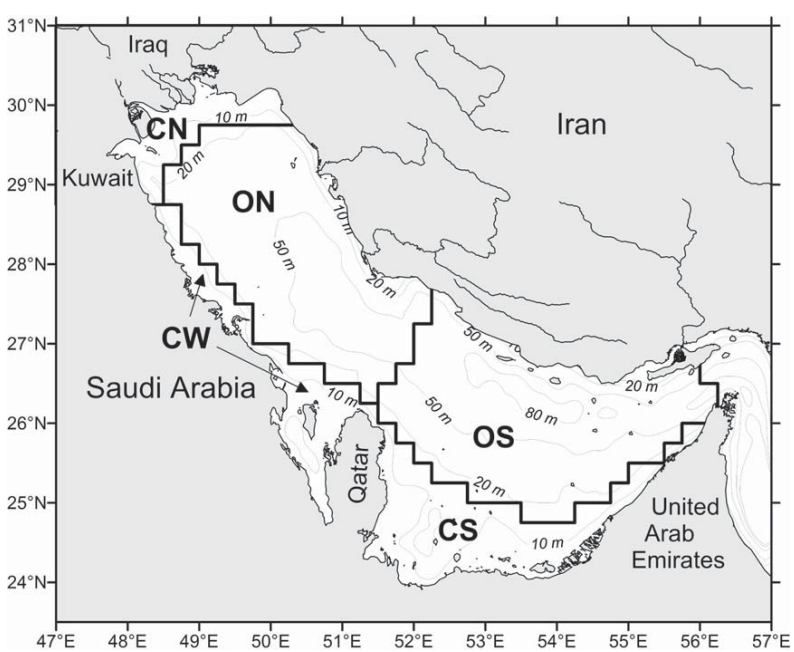

Fig. 1. Bathymetric map of the Arabian (Persian) Gulf and the analyzed regions: northern (ON) and southern (OS) open Gulf regions; coastal northern zone of Shatt Al-Arab plume (CN), coastal western zone along the Saudi coast (CW); and shallow area between Qatar and the United Arab Emirates Coast (CS).

Author's personal copy

the number of dust storms was assessed at nearly 27 per year (Safar, 1985). Dust storms are especially intensive in May–July (Pease et al., 1998) under the powerful northwesterly winds, when dust deposition can be as high as >30 g m^{-2} (Subba Rao and Al-Yamani, 1999b).

Sheppard (1993) attributes the Gulf to "one of the most productive bodies of water in the world", though statements of this kind should apply to benthic rather than pelagic production, because most of the area bed lies within the illuminated region. Subba Rao and Al-Yamani (1999a) demonstrated that the light levels at the bottom for the most part of Kuwait coastal waters were up to 83–275 W m^{-2}, i.e., sufficient for algal growth, and concluded that the Gulf algae are not light-limited most of the time. Vertical distribution of phytoplankton in the Gulf is characterized by comparatively low biomass at the surface and a pronounced subsurface maximum (Subba Rao and Al-Yamani, 1999a). The northern part of the Gulf is characterized by higher primary production and lower phytoplankton species diversity as compared with the south (Subba Rao and Al-Yamani, 1998).

We analyzed separately the five non-rectangular regions of the Gulf (Fig. 1), selected on the basis of bathymetry and known circulation patterns (see Reynolds, 1993): the northwestern shallow coastal zone influenced by Shatt Al-Arab plume (CN); the western shallow zone along Saudi coast (CW); the zone of "Southern Shallows" (CS) to the east of Qatar along the United Arab Emirates coast; the northern (ON) and southern (OS) "open" relatively deep regions with an eastern boundary at 56°E–56°15′E and the boundary between ON and OS about 51°30′E–52°15′E (northeast of Qatar). The boundary between ON and OS separates the regions different in water column stratification, which, according to previous studies (Brewer and Dyrssen, 1985; Reynolds, 1993; Swift and Bower, 2003), is high all year round in the OS and exhibits pronounced seasonal variability (maximum in summer) in the ON.

3. Materials and methods

The analysis presented in this paper is based on the data collected by several satellite sensors. Remotely-sensed CHL (mg m^{-3}) was measured by SeaWiFS aboard OrbView-2 platform (September 1997–February 2009) and MODIS aboard Aqua platform (July 2002–February 2009). The Level 3 Standard Mapped Images (SMI) were obtained from the NASA GSFC Distributed Active Archive Center (DAAC) (Acker et al., 2002). The format of Level 3 SMI is a regular grid of equidistant cylindrical projection of 360°/4096 pixels (about 9.28-km resolution) for SeaWiFS and 360°/8192 pixels (about 4.5-km resolution) for MODIS-Aqua. The basic algorithm used at GSFC for calculating CHL was described by O'Reilly et al. (1998). For each monthly composite, CHL and other parameters (aerosols, SST, etc.) in each of the five regions (Fig. 1) were averaged as a median. We used medians rather than arithmetic means because medians are more robust with respect to outliers and closer to modal values regardless of statistical distribution. In particular, statistical distributions of remotely-sensed chlorophyll (Banse and English, 1994; Campbell, 1995) and aerosol optical depth (O'Neil et al., 2000) are typically lognormal rather than normal. The pixels which didn't pass cloud test were eliminated from the SeaWiFS and MODIS observations (i.e., masked as "missing data", MD) during processing at GSFC. In monthly composites, the percentage of these pixels was relatively low (Table 1). In shallow regions (CN, CW, and CS), the percentage of MD pixels was higher than in open Gulf waters (ON and OS). Higher percentage of MD pixels in MODIS-Aqua data as compared with SeaWiFS could be explained by higher spatial resolution of MODIS-Aqua Level 3 grids (4.5 km vs. 9.28 km) and by better cloud screening for MODIS because of the use of thermal IR bands.

Only SeaWiFS data were used for time-series analysis from September 1997 to June 2002, i.e., before MODIS-Aqua data acquisition started; from July 2002 the SeaWiFS and MODIS-Aqua CHL for each month in each region were averaged. Comparison between SeaWiFS and MODIS-Aqua CHL products is beyond the scope of this study. For the open Gulf regions (ON and OS) and southern coastal region CS the logarithms of CHL monthly medians derived from SeaWiFS and MODIS-Aqua data were highly correlated ($R^2 = 0.74$–0.84) without an evident bias. In northern and western coastal regions, the correlation was lower ($R^2 = 0.34$–0.55).

Table 1
Percentage of pixels masked due to cloud cover (median, first and third quartiles) in SeaWiFS and MODIS-Aqua CHL data over the entire Gulf and in five Gulf regions: open northern (ON) and southern (OS), coastal northern zone of Shatt Al-Arab plume (CN), coastal western zone along the Saudi coast (CW); and shallow area between Qatar and the United Arab Emirates Coast (CS).

Region	SeaWiFS (pixel size 9-km)			MODIS-Aqua (pixel size 4.5-km)		
	Median (%)	Q1 (25%) (%)	Q3 (75%) (%)	Median (%)	Q1 (25%) (%)	Q3 (75%) (%)
ON	3.0	2.3	6.1	10.3	7.7	12.8
OS	4.5	3.0	6.1	16.7	15.4	19.2
CN	12.9	5.3	25.8	41.0	23.1	71.8
CW	8.3	4.5	20.5	19.2	15.4	37.2
CS	7.6	5.3	15.2	23.1	17.9	35.9
Total	4.5	3.0	8.3	16.7	11.5	21.8

Analyzing CHL derived from ocean color measurements collected from earth-orbiting satellite platforms, we do not compare the remotely-sensed CHL data to *in situ* chlorophyll *a* concentration and phytoplankton biomass, because for our analysis the absolute values are not as important as spatial and temporal gradients. One should keep in mind that remotely-sensed CHL may be subject to significant inaccuracies in the Gulf area. The standard SeaWiFS and MODIS CHL algorithms were developed for clean open ocean waters (Case 1), where the color of ocean surface results mainly from chlorophyll concentration (Morel and Prieur, 1977). Shallow regions of the Gulf, especially influenced by Shatt Al-Arab River discharge (CN, CW and CS), belong to coastal (Case 2) waters, where the ocean color is affected by the dissolved and suspended matter which may not be correlated with chlorophyll. Standard algorithms developed for open ocean (Case 1) may overestimate chlorophyll concentration in Case 2 waters (e.g., Muller-Karger et al., 2005). Another important factor leading to the overestimation of the remotely-sensed CHL in shallow waters is bottom reflectance which depends on bathymetric depth and water transparency (e.g., Maritorena et al., 1994).

In optically deep Gulf waters (ON and OS), the accuracy of assessment of phytoplankton biomass on the basis of remotely-sensed CHL can be limited by vertical distribution of phytoplankton. In the Gulf, vertical profiles of phytoplankton are often characterized by low concentration in the upper 5–10-m layer (Sheppard, 1993; Subba Rao and Al-Yamani, 1998), resulting in underestimation of total phytoplankton biomass derived from remotely-sensed CHL.

SeaWiFS observations of PAR (Einstein m^{-2} day^{-1}) (Frouin et al., 2001) and aerosol optical depth (thickness) at 865 nm (T865, unitless) and Ångström exponent at 510–865 nm (A510, unitless) were obtained from GSFC DAAC, also in the form of Level 3 SMI files of 9.28-km resolution. T865 and A510 are by-products of atmospheric correction in SeaWiFS ocean color data processing (Gordon and Wang, 1994; Gordon, 1997). Only the data measured over the ocean were used in this study. Retrievals of aerosol characteristics over the ocean are more accurate than over land, because the ocean surface has a relatively low and constant albedo (Husar et al., 1997; Li et al., 2009). However, the quality of some aerosol data collected over the shallow Gulf regions (attributed to Case 2 waters) was expected to be lower than over Case 1 (open ocean) due to higher and more variable water surface reflectance (e.g., Siegel et al., 2000).

SeaWiFS aerosol data were complemented by those measured by MODIS-Terra, which has shorter observation period (since 2000) but are expected to be more accurate due to using multi-channel information including several infrared bands (cf. Kinne et al., 2003).

Author's personal copy

Using CHL and aerosols measured by the same sensor (SeaWiFS) may result in erroneous correlations, since the derived aerosol properties are used for atmospheric correction for ocean color (e.g., Gordon and Wang, 1994). Also, SeaWiFS is lacking thermal infrared bands, thus significantly complicating separation of aerosol from cloud. As a result, very thick aerosols such as dust storms are usually masked out as clouds and aerosol optical depth retrieved by SeaWiFS is generally lower than by other satellite sensors (Myhre et al., 2005). MODIS-Terra aerosol data, including aerosol optical depth at 550 nm (T550) and Ångström exponent over ocean at 550–865 nm (A550), were obtained from GIOVANNI website (Acker and Leptoukh, 2007) in the form of monthly maps at 1°×1° spatial resolution. These data were interpolated over 0.1°×0.1° grids and converted to time series by integration over the two open Gulf regions (ON and OS). Recall that MODIS aerosol data used here were produced by MODIS aerosol team using aerosol-over-ocean algorithms (Tanre et al., 1997; Remer et al., 2005). These data are different from SeaWiFS-like aerosol products generated from MODIS radiances by the Ocean Biology Processing Group at NASA/GSFC led by C. McClain and G. Feldman. The latter aerosol product (not used in this study) is expected to be subject to the same methodological differences as the SeaWiFS aerosol product (i.e., masking high aerosol optical depth events as clouds thus leading to a low bias in the resulting averaged products).

We do not compare SeaWiFS and MODIS aerosols, because the aerosol products derived from different satellites exhibit significant differences, resulting from different sensors' wavelengths, spatial and temporal heterogeneity of aerosols, contamination by cloud and different treatments of surface reflectance in the retrieval algorithms, which is particularly important in the coastal regions (see Kinne et al., 2003; Myhre et al., 2005). Different sampling and data processing and averaging methodologies also contribute to products differences (e.g., Ignatov et al., 2006; Levy et al., 2009).

Sea surface temperature (SST, degrees C) data were based on the Advanced Very High Resolution Radiometer (AVHRR) infrared measurements obtained from NASA Jet Propulsion Laboratory Physical Oceanography Distributed Active Archive Center (NASA JPL PODAAC) and MODIS (Terra and Aqua) data obtained from GSFC DAAC. The AVHRR data were produced at JPL within the scope of National Oceanic and Atmospheric Administration (NOAA)/NASA AVHRR Oceans Pathfinder Project using state-of-the-art SST algorithms (Walton, 1988; Kilpatrick et al., 2001). The data format of Pathfinder Version 5 is a quasi-regular grid of approximately 4.5-km resolution. We used monthly data of both ascending and descending satellite passes (i.e., daytime and nighttime observations, respectively). Only the data with quality flags 4–7 (i.e., the "best SST") were used. MODIS SST data format is similar to MODIS CHL. For MODIS, all three available SST data sources were used: daytime (SST) and nighttime (NSST) data based on 10-μm waveband and nighttime data based on 4-μm waveband (SST4), from both Terra and Aqua. For each month, all available SST data were averaged (as arithmetic means of up to eight SSTs). Standard deviation of averaging was 0.77–1.01 °C in open Gulf regions and 1.05–1.35 °C in coastal regions.

For wind speed, we used NCEP/NCAR reanalysis monthly data (Kalnay et al., 1996) of 2.5°×2.5° spatial resolution. Each monthly grid of scalar wind speed was averaged (as a median) over the entire Gulf.

Seasonal variations of all aforementioned variables were analyzed from their climatologies, calculated as medians of calendar months. To analyze interannual variability, each parameter was transformed to seasonal anomalies by subtracting their respective climatic monthly values. CHL anomalies were calculated from log-transformed data and the result was exp-transformed back to CHL concentration. Thus the resulting CHL seasonal anomalies represent the ratio between the observed and climatic values rather than the difference and, as such, are unitless.

Annual precipitation in the area surrounding the Gulf (22.5°N–35°N; 45°E–57.5°E) was calculated from the data obtained from the Global Precipitation Climatology Project (GPCP) website. The data format was global monthly grids of 2.5°×2.5° spatial resolution. Precipitation in the Gulf region was averaged annually over 12-month periods from July to June. GPCP data are based on the measurements collected by different satellites (see Huffman et al., 2001). In arid regions, monthly averaged GPCP data are well correlated with rain-gauge data (e.g., Nezlin and Stein, 2005) and can be used in the areas where rain-gauge data are unavailable or unreliable because of small number of rain-gauge stations. At the same time, one should take into account that in semiarid climates GPCP data may be overestimated as compared with rain-gauge data due to rainfall evaporation (see Marcella and Eltahir, 2008).

To relate the interannual variations of precipitation over the Gulf to the global climatic meteorological cycles, we used North Atlantic Oscillation (NAO) index, obtained from the NOAA Earth System Research Laboratory website (http://www.cdc.noaa.gov/data/climateindices/) and Indian Ocean Dipole Mode Index (DMI), obtained from the UNESCO website (http://ioc3.unesco.org/oopc/). NAO is defined as the monthly averaged difference between the standardized measurements of the sea level atmospheric pressure in Azores Islands and Iceland. During positive/negative NAO, the storm tracks over western Eurasia (including Middle East) are shifted northward/southward (Rodionov, 1994), affecting local meteorological conditions and water balance (Cullen et al., 2002). DMI is an indicator of the east–west temperature gradient across the tropical Indian Ocean (Saji et al., 1999). The periods of persistently high DMI are associated with extreme rainfall in the western Indian Ocean region (Ashok et al., 2001; Black et al., 2003).

4. Results

4.1. Seasonal variability

Seasonal CHL cycle in the open Gulf waters was characterized by winter maximum and summer minimum (Fig. 2A), which is typical to subtropical ocean (Longhurst, 1995). No significant difference was found between the northern and southern parts of open Gulf waters all year round except July. This similarity looks surprising, because according to published data the two regions have substantial differences in hydrology: water column in the northern deep region is stratified during summer and mixed during winter while in the southern deep region water column is stratified all year round (Brewer and Dyrssen, 1985; Reynolds, 1993; Swift and Bower, 2003).

In July, CHL in the open south region (OS) was substantially higher than in the north (ON); this difference can be attributed to the inflow of Indian Ocean surface waters (IOSW) through the Strait of Hormuz. IOSW influence the OS area to southeast of Qatar all year round. IOSW form a cyclonic gyre in the southern half of the Gulf during winter and penetrate further to the north during summer (Abdelrahman and Ahmad, 1995). From spring to autumn, the productivity of IOSW increases as a result of seasonal upwelling in the Arabian Sea forced by southwesterly monsoon (e.g., Levy et al., 2007), and the southern part of the Gulf was likely affected by this increase more than the northern one.

In the shallow northern part of the Gulf (CN, the Shatt Al-Arab plume zone), CHL was much higher than in the other regions (Fig. 2B) throughout the year, with minimum in summer. This minimum was not observed in *in situ* observations during the period March 1997 through April 1998, which demonstrated no pronounced seasonal pattern of chlorophyll concentration off Kuwait except in the northern stations where maximum values (<20 mg m^{-3}) in March–July were associated with seasonal maximum of Shatt Al-Arab nutrient-rich discharge (Al-Yamani et al., 2006). The distorted seasonal signal in remotely-sensed CHL could be due to overestimation of remotely-sensed CHL signal by bottom reflection, which was high from autumn to spring when water was clean. The effect of bottom reflectance was suppressed in the summer, when water turbidity was high.

Author's personal copy

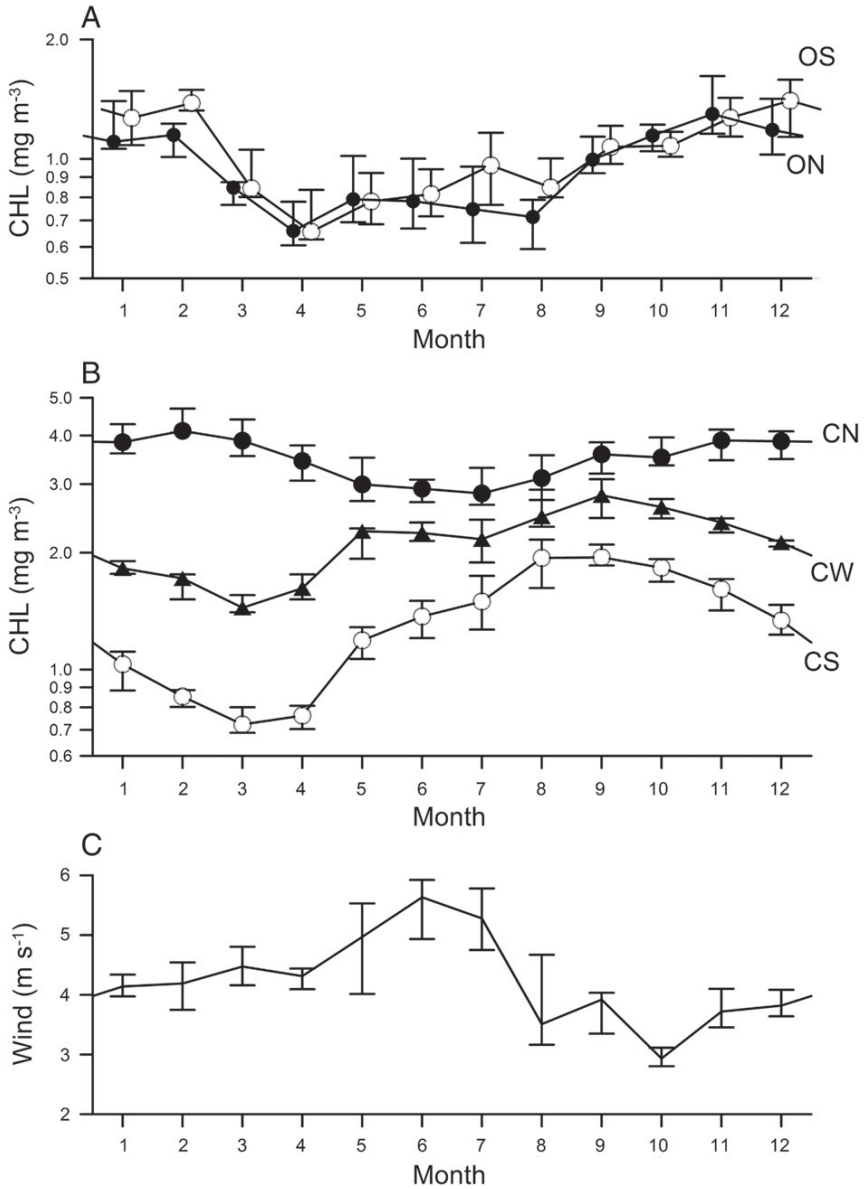

Fig. 2. Seasonal variations of CHL in northern (solid circles) and southern (open circles) open Gulf regions (A) and in northern (solid circles), western (triangles) and southern (open circles) coastal regions (B); NCEP wind speed over the Gulf (C). Climatology was calculated as monthly medians over 1997–2008; vertical error bars indicate first and third quartiles. The temporal offset in Panel A was made to help distinguish between the OS and ON time series.

In western (CW) and southern (CS) shallow regions, the minimum of CHL was observed in spring (February–April) and maximum in late summer and autumn (August–October; Fig. 2B). These maxima coincided with the seasonal minimum of wind mixing over the Gulf (Fig. 2C) suggesting that in shallow waters turbidity decreased and bottom reflectance increased. We conclude that in shallow Gulf regions bottom reflectance signal was substantial and remotely-sensed CHL data were significantly and irregularly overestimated. We keep in mind, however, that sediments resuspended by wind provide a non-linear effect on remotely-sensed CHL measurements. On the one hand, in the regions where remotely-sensed CHL is significantly obscured by bottom reflectance (cf. Maritorena et al., 1994), suspended sediments decrease the contribution of the bottom optical signal decreasing CHL measured by satellites. On the other hand, resuspension of chlorophyll off the seafloor can be misinterpreted as a bloom when seen in satellite color imagery (Wynne et al., 2006). Unrealistic seasonal cycles of CHL in all three shallow Gulf regions (CN, CW and CS) seemingly associated with turbidity and bottom reflectance rather than seasonal dynamics of phytoplankton biomass indicate that these data are inaccurate and their interannual variability should be excluded from further analysis. In "optically shallow" Gulf waters, ocean color satellite imagery should be processed using special algorithms allowing for bottom reflectance (e.g., Cannizzaro and Carder, 2006); this approach will be a focus of our future studies. In the present study, based on Level 3 ocean color data processed by standard method, we focus on CHL dynamics only in optically deep open Gulf regions ON and OS.

The seasonal patterns of SST (estimated from remotely-sensed infrared data) were similar in all Gulf regions (not shown) and demonstrated a significant range of variability (cf. Sheppard, 1993), with late winter minimum (from ~17 °C in CN to ~20 °C in OS regions) and late summer maximum (33–34 °C). Similarity between

Author's personal copy

the SST seasonal patterns in the northern and southern Gulf (as well as CHL) can be explained by intensive horizontal circulation throughout the Gulf area. During spring and summer, a cyclonic overturning circulation is established along the entire Gulf; during autumn and winter, this circulation breaks up into mesoscale eddies, laterally stirring most of the Gulf's surface waters (Sadrinasab and Kampf, 2004).

The seasonal patterns of aerosol optical depth and Ångström exponents were similar over northern and southern Gulf waters (Fig. 3). Aerosol optical depth was low during winter (November–March) and increased during summer with maxima in July and August. At the same time, Ångström exponents showed a pronounced minima in May–July, when aerosols were dominated by large particles of aeolian dust (note that this period also coincided with maximum of wind speed; Fig. 2C). These seasonal patterns are well known for desert areas including Middle East (Husar et al., 1997). We have to keep in mind, however, that during intensive winds large-size aerosols over sea surface (including the Gulf) might result not only from aeolian dust but also from sea salt aerosols produced by bursting of bubbles formed by breaking waves and mechanical disruption of wave crests (Mulcahy et al., 2008; Huang et al., 2009; Lehahn et al., 2010).

The absolute values of aerosol optical depths and Ångström exponents estimated by MODIS-Terra and SeaWiFS agree only qualitatively but significantly differ quantitatively, due to large differences in the processing algorithms, especially cloud screening, and different wavelengths employed by the two sensors (see Myhre et al., 2005). The MODIS aerosol product is expected to be more accurate, although it also shows some artifacts. In particular, the decrease of T550 in Fig. 3B in June in the northern Gulf coincided with the period of most intensive dust storms (which mostly affected northern Gulf), possibly due to some elevated aerosol data misclassified as clouds and eliminated.

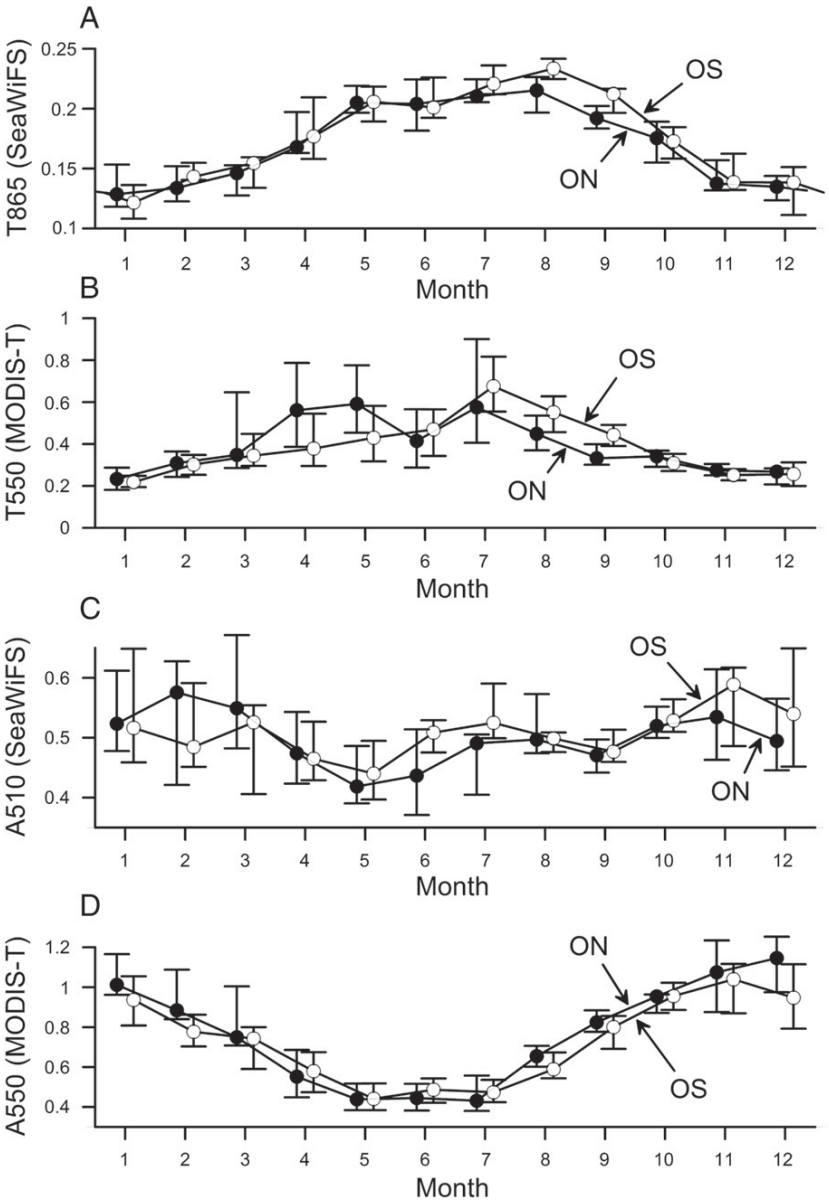

Fig. 3. Seasonal variations of aerosol optical depth at 865 nm measured by SeaWiFS (A) and at 550 nm measured by MODIS-Terra (B); Ångström exponent at 510 nm measured by SeaWiFS (C) and at 550 nm measured by MODIS-Terra (D) in northern (solid circles) and southern (open circles) open Gulf regions. Climatology was calculated as monthly medians over 1997–2008; vertical error bars indicate first and third quartiles. The temporal offset was made to help distinguish between the OS and ON time series.

Author's personal copy

4.2. Interannual variability

At interannual scale, CHL anomalies in open Gulf waters were characterized by a positive trend (Fig. 4A). In 1997–1999, CHL anomalies were mostly negative; in 2000–2002 and 2007–2008, positive anomalies dominated. Similar increasing trends were demonstrated on the basis of SeaWiFS CHL in many coastal regions of the World Ocean (Kahru and Mitchell, 2008). At the same time, CHL and aerosol retrievals are known to be very sensitive to radiometric uncertainties (Gordon et al., 1983; Evans and Gordon, 1994; Ignatov, 2002). As a result, their long-term trends may be affected by small radiometric changes in SeaWiFS and MODIS. These trends are irrelevant for this study which concentrates on large-scale year-to-year variability and therefore are not analyzed here.

Anomalously high CHL was observed in both northern and southern Gulf regions in summer 2000 (from May to September), when CHL exceeded the climatic concentration by a factor of 1.5 and in winter 2008–2009 (October–January) in southern Gulf, where CHL was higher than normal by a factor >3. The bloom in summer 2000 was characterized by high CHL over the entire Gulf area as well as in the adjacent Arabian Sea (Patra et al., 2007). In autumn 2008, very intensive bloom started in the Strait of Hormuz and spread to the Gulf along the Iranian coast (Fig. 5). Harmful algal blooms with fish mortality were reported in the Iranian (close to the Strait of Hormuz/Hormuzgan), United Arab Emirates (southern Gulf waters and northern Gulf of Oman), and the Omani waters (Gulf of Oman) starting September 2008 and continued for several months (ROPME, 2009). Both years 2000 and 2008 were characterized by very low precipitation (Fig. 4B) and high concentration of large aerosols, i.e., high aerosol optical depth and low Ångström coefficient (Fig. 6), indicating high concentration of large aerosol particles, supposedly desert dust, transported by wind over the Gulf surface. In 1999–2000, low precipitation coincided with higher than normal NAO index (Fig. 4C). In 2000, low A550 was evident only in the southern OS region, while A510 exhibited a pronounced minimum.

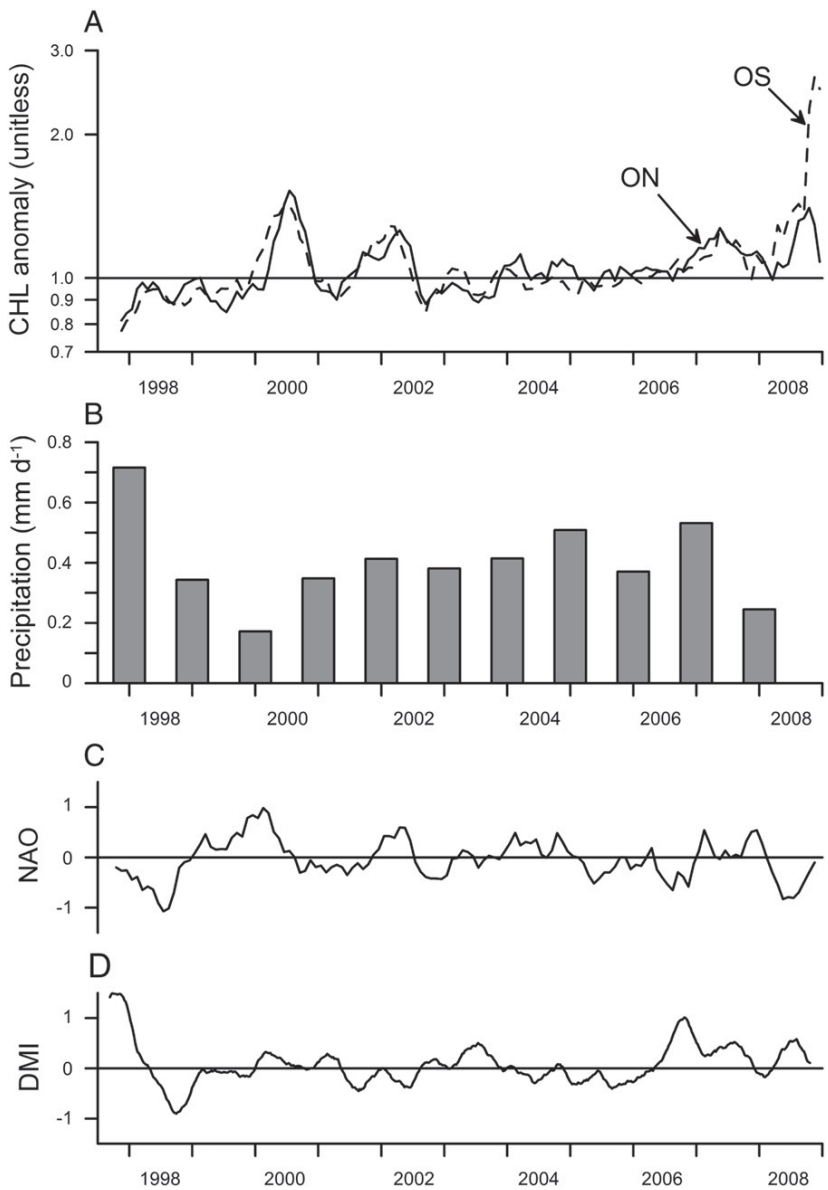

Fig. 4. Interannual variations of CHL seasonal anomalies (smoothed by 5-month running average) in northern (solid line) and southern (dashed line) open Gulf regions (A); atmospheric precipitation over the area surrounding the Gulf (22.5°N–35°N; 45°E–57.5°E); North Atlantic Oscillation index (NAO; C) and Indian Ocean Dipole Mode Index (DMI; D). Note that CHL seasonal anomalies (unitless) represent the ratio between the observed and climatic values.

Author's personal copy

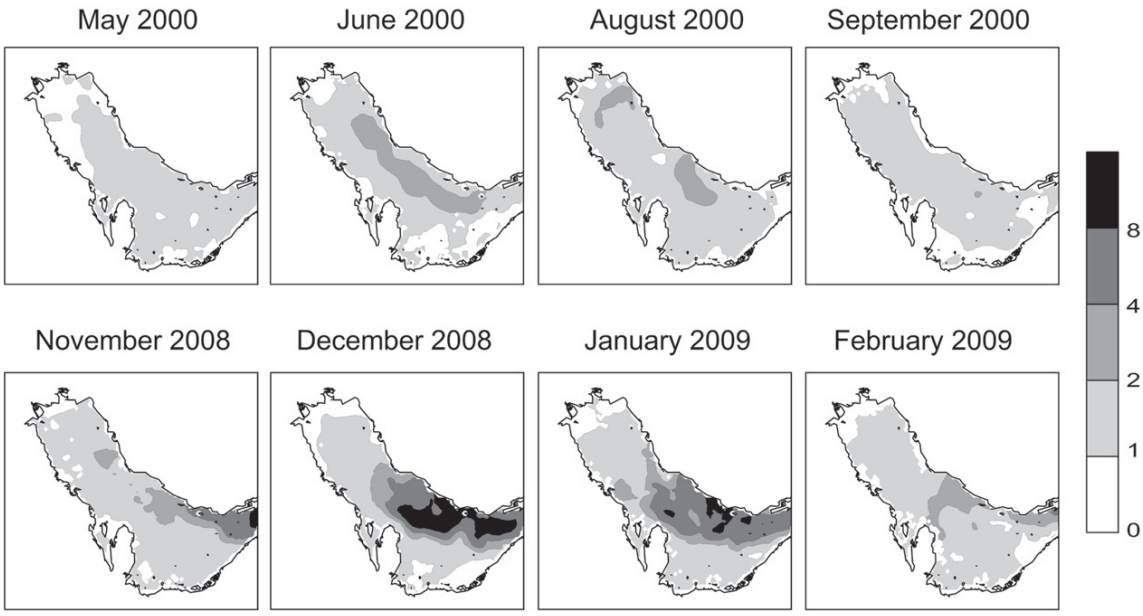

Fig. 5. CHL anomalies (the ratio between monthly and climatic, unitless) observed by SeaWiFS during the blooms in May–September 2000 and November 2008–February 2009. The grids of 9.28-km resolution were smoothed by 5×5 filter.

In 2008, only A550 (measured by MODIS) was negative, while A510 (measured by SeaWiFS) was positive, which could be attributed to its low accuracy, i.e., dust storm events masked as "clouds" and eliminated from the analysis.

We suggest that in 2000 and 2008 low precipitation resulted in higher than normal dust transport over the Gulf. First, aeolian erosion in the desert areas surrounding the Gulf was high due to lower than normal soil moisture (cf. Mahowald et al., 2005). Second, precipitation is an important process for cleaning the atmosphere of trace constituents like aerosols through nucleation scavenging and Brownian diffusion or impaction scavenging (Bergametti et al., 1992; Praveen et al., 2007). At the same time, high aerosol optical depth during extremely dry periods of 2000 and 2008 could be partly attributed to fewer clouds, which in turn would lead to better aerosol sampling of larger optical depth values.

No significant light limitation of phytoplankton growth was observed in the Gulf. The correlation between phytoplankton biomass (i.e., CHL anomalies) and PAR anomalies was low and observed only in the northern Gulf (ON; Table 2). In the southern Gulf (OS), CHL was not correlated with PAR, indicating that most phytoplankton was concentrated in the euphotic zone and photosynthesis was not light-limited, which was noted earlier by Subba Rao and Al-Yamani (1999a). PAR was close to normal during the blooms of 2000 and 2008 (not shown).

The SST interannual variations were identical in both open Gulf regions (ON and OS; Fig. 7B), demonstrating intensive horizontal mixing throughout the Gulf. In 2000 and 2008, SST was close to its climatological background (Fig. 7B), suggesting that both phytoplankton blooms (in 2000 and 2008) were not associated with intensification of upwelling or vertical mixing of water column. Also, no significant correlation was found between CHL and wind speed anomalies. Minor role of the factors associated with water column stratification indicates other factors regulating phytoplankton growth in the Gulf and indirectly supports the hypothesis of ocean fertilization by aeolian dust transport.

The analysis of the entire observed period revealed low but significant negative correlation between CHL and SST anomalies (Table 2). This correlation (i.e., simultaneous decrease of SST and increase of remotely-sensed CHL) may be explained by different processes. First, the open Gulf waters are well stratified (Sultan and Elghribi, 1996; Abdelrahman, 1998; Swift and Bower, 2003) and a decrease in SST looks like a surface signature of vertical mixing and/or upwelling stimulating phytoplankton growth. Second, low SST can be associated with increased dust transport, because negative effect of dust on SST can be explained by attenuation of surface shortwave radiation (Foltz and McPhaden, 2008). Singh et al. (2008) pointed out that dust storms are associated with high wind speed and both factors (dust fertilization and water column mixing) could work in parallel stimulating phytoplankton growth. Third, in the Gulf waters, phytoplankton is often concentrated in subsurface layer (Sheppard, 1993; Subba Rao and Al-Yamani, 1998) and vertical mixing could transport phytoplankton cells to the surface, resulting in more intensive CHL signal observed by satellites immediately after storm event. All three processes would result in correlation between SST and CHL at a monthly time scale. At the same time, at daily time scale these processes could be distinguished, because phytoplankton growth stimulated by nutrient input (by either water column mixing or dust deposition) is expected after a few days (up to 1 week) after the impact (Cropp et al., 2005; Volpe et al., 2009). The analysis based on daily satellite imagery would be a focus of our future studies.

In 1997–1999, negative CHL anomalies (Fig. 4A) coincided with positive SST anomalies (Fig. 7B). The 1998–1999 warm event in the Gulf followed the 1997–1998 El-Niño event, strongest in the XX century (McPhaden, 1999), coinciding with high temperature in western Indian Ocean (see DMI index; Fig. 4D). Significant effect of this warming on corals was well documented in the Gulf (Riegl, 2002) and the surrounding ocean areas (Goreau et al., 2000). In the Gulf area, the warming event was associated with higher than normal precipitation (Fig. 4B), sluggish wind (Fig. 7A), and lower than normal PAR (not shown) and CHL (Fig. 4A). Aerosol properties measured by SeaWiFS (T865 and A510; Fig. 6A, C) indicated low concentration of large aerosols, supporting the hypothesis of phytoplankton fertilization by desert dust deposition.

Additional arguments supporting the hypothesis of dust fertilization were positive correlation between CHL and aerosol optical depth (T865 and T550) and negative correlation between CHL and Ångström exponent A550 (Table 2). At the same time, the correlation between

Author's personal copy

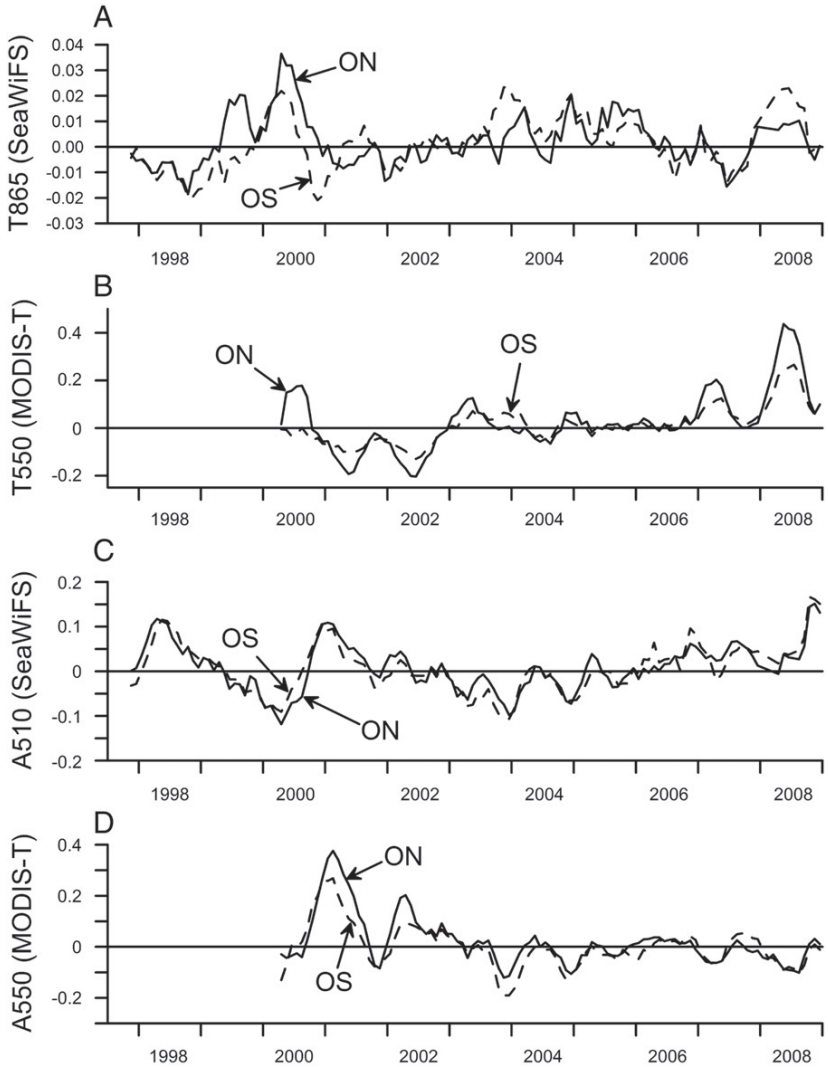

Fig. 6. Interannual variations of seasonal anomalies (smoothed by 5-month running average) of aerosol optical depth at 865 nm measured by SeaWiFS (A) and at 550 nm measured by MODIS-Terra (B); Ångström exponent at 510 nm measured by SeaWiFS (C) and at 550 nm measured by MODIS-Terra (D) in northern (solid line) and southern (dashed line) open Gulf regions.

CHL and the Ångström exponent measured by SeaWiFS (A510) was positive; the latter disagreement can be explained by low (as compared with MODIS) accuracy of SeaWiFS aerosol measurements (cf. Tanre et al., 1997; Remer et al., 2005) and contamination of ocean color signal by absorbing aerosols resulting in overestimation of CHL (cf. Moulin et al., 2001; Claustre et al., 2002; Ransibrahmanakul and Stumpf, 2006).

5. Discussion

The results of this study suggest that the intensity of aeolian dust deposition (supposedly associated with iron micronutrient) may play an important role as a factor regulating phytoplankton variability in the Gulf. This relationship was especially evident on interannual scale:

Table 2
Time-lagged correlations (R) between the seasonal anomalies of CHL (log-transformed; SeaWiFS + MODIS-Aqua) and the seasonal anomalies of PAR, SST, T865, T550, A510, and A550 in northern (ON) and southern (OS) Gulf regions. Positive time lag means that the environmental variable leads CHL. All coefficients are significant at 95% confidence level.

Parameter	Satellite	Period	ON		OS	
			R	Time lag	R	Time lag
PAR	SeaWiFS	September 1997–December 2008	+0.265	+7	–	–
SST	AVHRR + MODIS-Terra	September 1997–December 2008	−0.219	+3	−0.211	+3
T865	SeaWiFS	September 1997–December 2008	+0.283	0	+0.332	+5
T550	MODIS-Terra	February 2000–December 2008	+0.309	+3	+0.418	+6
A510	SeaWiFS	September 1997–December 2008	–	–	+0.331	0
A550	MODIS-Terra	February 2000–December 2008	−0.221	+3	−0.216	+3

Author's personal copy

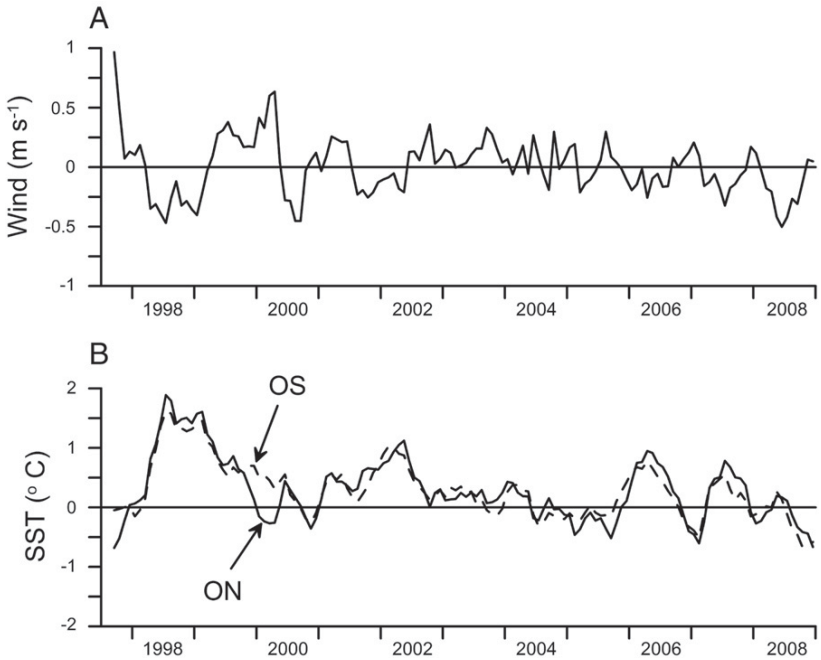

Fig. 7. Interannual variations of seasonal anomalies (smoothed by 5-month running average) of wind speed (A) and sea surface temperature (B). Wind over the entire Gulf area; SST in northern (solid line) and southern (dashed line) open Gulf regions.

two extremely dry periods in 2000 and 2008 were associated with dense large-particle aerosols and followed by phytoplankton blooms.

Proposing the hypothesis of iron fertilization, we attribute the Gulf to the regions where phytoplankton growth is iron-limited. Iron limitation was observed in many ocean regions (Martin et al., 1991, 1994; Coale et al., 1996; Sunda and Huntsman, 1997) and aeolian dust was indicated as an important source of this micronutrient (Betzer et al., 1988; Neuer et al., 2004; Jickells et al., 2005; Chase et al., 2006; Walsh et al., 2006; Chen et al., 2007). Dust fertilization of phytoplankton growth was illustrated by experiments (Subba Rao and Al-Yamani, 1999b; Mackey et al., 2007) and direct observations of phytoplankton blooms following dust storms (Martin et al., 1989; Guerzoni et al., 1999; Meskhidze et al., 2005; Singh et al., 2008). In coastal regions, atmospheric deposition of iron can result in harmful algal blooms (Paerl, 1997; Walsh et al., 2006). Recent studies demonstrated non-linear effect of aerosols on the growth of different phytoplankton species: not all aerosols stimulated phytoplankton growth; some aerosols (e.g., originating from Sahara Desert) produced toxic effect supposedly associated with high copper concentration (Paytan et al., 2009). Negative effect of dust on primary production may also result from light attenuation (Mallet et al., 2009).

In the Gulf, the effect of aeolian dust transport on phytoplankton growth might be stronger than in other ocean regions, because the land areas surrounding the Gulf are among the main sources of aeolian dust in the world (Husar et al., 1997) and iron concentration in aerosols in this region is comparatively high (Patra et al., 2007). Previous studies indicated that dust produced in deserts, especially by the soils in the Tigris and Euphrates basin, is transported by northwesterly Shamal winds to the Gulf and further to the Arabian Sea (Husar et al., 1997). Aeolian activity in the southern Iraq and Kuwait dramatically increased between 1989 and 1992, which was attributed to the disruption of desert surface due to the Gulf War (Al-Dabi et al., 1997).

Analyzing the relationship between aerosols and CHL, it is important to distinguish between the effect of dust fertilization on phytoplankton growth and the optical effect of dust on CHL retrieval (cf. "Artifact" hypothesis in Cropp et al., 2005). In this study, we explore the hypothesis that the observed relationship between aerosol properties and CHL over the open Gulf waters resulted from iron fertilization. At the same time, we cannot completely rule out the possibility that high CHL measured by satellites partly resulted from the optical effect of dense aerosols. Previous studies demonstrated that dust and some other aerosols (soot, smoke, air pollution, etc.) in the atmosphere or in the near-surface water absorb blue light corrupting remotely-sensed signal and resulting in overestimation of CHL (Moulin et al., 2001; Claustre et al., 2002; Ransibrahmanakul and Stumpf, 2006). Positive correlations with zero time lag between CHL and aerosol characteristics (optical depth T865 and Ångström exponent A510) derived from SeaWiFS measurements (Table 2) can be attributed to this effect. However, the blooms in the Gulf did not coincide with the periods of intensive dust storms but followed them after a certain time lag, indicating dust fertilization rather than an "Artifact" in CHL retrieval. This conclusion corroborates well with previous studies. Claustre et al. (2002) and Volpe et al. (2009) demonstrated that overestimation of remotely-sensed CHL (by a factor of 2) occurred mostly in chlorophyll-poor waters, which was not the case in chlorophyll-rich Gulf. Cropp et al. (2005) rejected the "Artifact" hypothesis on the basis of the absence of a widespread bias in SeaWiFS CHL products. Similar conclusion by Erickson et al. (2003) was based on displacement of the areas of high chlorophyll as compared to aeolian iron flux due to horizontal ocean transport.

Time lags between aerosols and CHL were observed at both seasonal and interannual time scales. Seasonal cycle of aerosol size spectra (A510 and A550) indicated maximum concentration of large particles in May–July, supporting the earlier observations that dust transport to the Gulf was strongest in early summer (Subba Rao and Al-Yamani, 1999b); elevated CHL was observed from September to February. During bloom events in 2000 and 2008, the aerosol properties characterizing intensive dust storms were observed in spring and early summer; at the same time, the phytoplankton blooms were observed later: during the summer–autumn of 2000 and the autumn–winter of 2008/2009. Previously, time lags between dust fertilization and phytoplankton blooms were shown in numerical experiments with different spatial patterns of dust deposition in the

Author's personal copy

Arabian Sea (Wiggert and Murtugudde, 2007) and satellite observations in the Mediterranean Sea (Guerzoni et al., 1999). In the Gulf, time lags between dust and CHL were observed during various seasons and could not be attributed to seasonal effects demonstrated in other ocean regions, including the Red Sea and Mediterranean (Herut et al., 2002; Markaki et al., 2003; Chen et al., 2007), where, in contrast, maximum effect of aeolian dust deposition on phytoplankton growth was observed during summer–autumn season, when water column was stratified and the contribution of nutrients from deeper layers was reduced.

The seasonal cycles of wind speed and CHL in the open Gulf waters do not correlate, indicating that wind mixing is not the primary factor regulating phytoplankton growth. The seasonal cycle of CHL was characterized by maximum in winter (November–February) and minimum in spring (April). Prima facie, this cycle looked like a nutrient-limited seasonal pattern typical to subtropical ocean, where phytoplankton biomass is negatively correlated to stratification enhanced by summer solar heating (resulting in sharp pycnocline and nutrient limitation) and eroded in winter by surface cooling and wind mixing (Longhurst, 1995). The effect of winter mixing on CHL was described by Levy et al. (2007) in the northern part of the Arabian Sea adjacent to the Gulf, where two seasonal maxima of comparable amplitude were observed: summer bloom driven by upwelling-favorable southwesterly monsoon and winter peak resulting from vertical mixing driven by northeasterly monsoon. However, in contrast to the Arabian Sea, the Arabian (Persian) Gulf is characterized by the absence of conventional biological seasonality. Previous studies in the Gulf (Sultan and Elghribi, 1996; Abdelrahman, 1998; Swift and Bower, 2003) indicated strong pycnocline (especially in its southern part in summer) resulting from both insolation of the surface and concentration of dense saline water in the bottom layer. In winter–spring, strong winds over the Gulf surface result not only in deepening of the upper mixed layer, but also stimulate deep mixing resulting from lower humidity and higher evaporation rates as compared with summer–autumn (Swift and Bower, 2003). However, these variations in wind speed do not affect CHL seasonal cycle, in contrast to adjacent deep ocean regions like the northern part of the Arabian Sea (cf. Levy et al., 2007). On the basis of small role of wind we hypothesize that the factor stimulating phytoplankton growth in the Gulf is aeolian dust transport which maximum in late spring–early summer triggers the growth of phytoplankton biomass.

The seasonal minimum of CHL in April may result from the seasonal maximum of Indian Ocean Surface Waters (IOSW) inflow into the Gulf (Swift and Bower, 2003). The productivity of these waters depends on upwelling in the Arabian Sea driven by monsoons, with minimum in winter–spring and maximum in summer–autumn. As such, the productivity of IOSW in April is still comparatively low and their influx can decrease CHL in productive Gulf waters. IOSW have salinity significantly lower than the Gulf waters they overflow. This vertical salinity gradient results in enhanced stratification (Swift and Bower, 2003), which can, on the one hand, contribute to nutrient limitation of phytoplankton growth and, on the other, confine vertical distribution of phytoplankton to deep subsurface maximum (Reynolds, 1993; Subba Rao and Al-Yamani, 1998), resulting in low remotely-sensed CHL.

One more argument indirectly supporting iron hypothesis is the fact that IOSW flowing into the Gulf are rich in phosphates but poor in nitrates (Brewer and Dyrssen, 1985). As such, they provide a good environment for diazotrophs (e.g., *Trichodesmium* spp.) that fix atmospheric nitrogen and have higher than other phytoplankton groups iron requirements (e.g., Walsh et al., 2006) thus increasing the effect of iron deposition on phytoplankton growth. This suggestion, however, should be supported by field data.

The differences between the magnitudes of the phytoplankton blooms in 2000 and 2008 could be attributed to the differences in aerosols. The bloom in 2008 was more extensive as compared with 2000. Most noticeable difference between the aerosol characteristics in 2000 and 2008 was Ångström exponent, which was low in 2000 but close to normal in 2008 suggesting that in 2008 aerosol particles were smaller than in 2000. Previous studies demonstrated that fine-mode aerosols tend to yield larger iron solubilities than coarse mode aerosols (Mahowald et al., 2005), which might have been the case in 2008. Solubility (and resulting bioavailability) of iron varies in different aerosols, dramatically increasing due to atmospheric processing (see Mahowald et al., 2005). In particular, an important factor affecting iron solubility (dissolved iron fraction) is dust acidification by sulfuric acid emitted to the atmosphere from both natural and anthropogenic sources (Meskhidze et al., 2005). Natural sources (~20%) include volcanic emissions and oxidation of biogenic dimethyl sulfide from the ocean; anthropogenic sources (~80%) include industrial emissions (especially metal production), liquid and solid fossil fuel combustion, biomass burning, and aircraft exhaust (Koch et al., 1999; Chin et al., 2000; Tegen et al., 2000).

It is possible that in 2000 and 2008, aerosols originated from different sources. This hypothesis is based on the differences in aerosol properties and NAO climatic index, high in the beginning of 2000 and low in mid-2008. During positive NAO, the mid-latitude westerly winds over the North Atlantic are strong and the storm tracks over western Eurasia are shifted northward (Rodionov, 1994). The decrease of precipitation in 2000 (but not in 2008) could be associated with these large-scale atmospheric circulation changes typical to positive NAO extreme. Low precipitation in 2008 was associated with negative NAO extreme, resulting in southward shift of storm tracks over Europe. In the Gulf area, this weather pattern was characterized by low wind. Another climatic cycle regulating precipitation over the western Indian Ocean is DMI, which positive extremes coincide with higher than normal SST and precipitation (e.g., 1997/1998 and 2006/2007). At the same time, in 2000 and 2008, when precipitation around the Gulf was low, DMI was close to normal.

Analysis in this paper was based on monthly Level 3 CHL satellite data processed at GSFC using standard algorithms. In the Gulf (as well as in similar coastal regions), remotely-sensed CHL is subject to substantial flaws, which should be addressed in future ocean color algorithms.

A significant part of the Gulf is covered by shallow waters with optical properties affected by bottom reflection. Processing satellite imagery collected over these waters, specific algorithms removing the bottom effect (e.g., Cannizzaro and Carder, 2006) should be used. Another source of data corruption is absorbing aerosols; the potential method of data correction is a spectral-matching algorithm (e.g., Banzon et al., 2004) increasing chlorophyll data recovery in areas otherwise masked by standard processing.

Remotely-sensed CHL and aerosol properties indicating aeolian dust transport should be compared to field data. Also, aerosol data collected by different satellites should be used, including Total Ozone Mapping Spectrometer (TOMS) Absorbing Aerosol Index (Torres et al., 1998).

Finally, future studies of phytoplankton variability in the Gulf and other regions affected by aeolian dust transport should be based on detailed analysis of the events documented by field data and satellite imagery of high spatial and temporal resolution. Similar studies in other regions (e.g., Meskhidze et al., 2005; Singh et al., 2008) revealed the patterns of phytoplankton blooms following dust storms indicating that under certain local conditions dust (iron) fertilization could be a significant factor regulating ocean productivity.

6. Conclusions

Seasonal and interannual variability of remotely-sensed chlorophyll in the Arabian (Persian) Gulf can be explained by local meteorological and oceanographic factors, including vertical stratification, precipitation, and aeolian dust transport. The periods of low

Author's personal copy

precipitation in 2000 and 2008 coincided with aerosol properties indicating elevated level of dust deposition over the Gulf surface and resulted in phytoplankton blooms in the open Gulf waters. Dust fertilization was suggested to be an essential factor regulating phytoplankton growth in the Gulf.

Acknowledgements

The authors would like to thank the SeaWiFS Project (Code 970.2) and the Distributed Active Archive Center (Code 902) at the NASA Goddard Space Flight Center for the production and distribution of remotely-sensed images, respectively. These activities are sponsored by NASA's Mission to Planet Earth Program. We also thank the NASA Physical Oceanography Distributed Active Archive Center at the Jet Propulsion Laboratory, California Institute of Technology for SST data. We are thankful for MODIS project for CHL and aerosol data and for NCEP/NCAR and GPCP for wind and precipitation data. We thank the team at NASA GES DISC developing and maintaining GIOVANNI online data system. The remarks of three unknown reviewers were extremely helpful and significantly improved the paper. The authors thank the Kuwait Institute for Scientific Research (KISR) for initiation and support of this study.

References

Abdelrahman, S.M., 1998. Seasonal variations of sound speed in the Arabian Gulf. Oceanologica Acta 21 (1), 59–68.
Abdelrahman, S.M., Ahmad, F., 1995. A note on the residual currents in the Arabian Gulf. Continental Shelf Research 15 (8), 1015–1022.
Acker, J.G., Leptoukh, G., 2007. Online analysis enhances use of NASA earth science data. EOS 88 (2), 14–17.
Acker, J.G., Shen, S., Leptoukh, G., Serafino, G., Feldman, G., McClain, C., 2002. SeaWiFS ocean color data archive and distribution system: assessment of system performance. IEEE Transactions on Geoscience and Remote Sensing 40 (1), 90–103.
Al-Dabi, H., Koch, M., Al-Sarawi, M., El-Baz, F., 1997. Evolution of sand dune patterns in space and time in north-western Kuwait using Landsat images. Journal of Arid Environments 36 (1), 15–24.
Al-Yamani, F., Subba Rao, D.V., Mharzi, A., Ismail, W., Al-Rifaie, K., 2006. Primary production off Kuwait, an arid zone environment, Arabian Gulf. International Journal of Oceans and Oceanography 1 (1), 67–85.
Ashok, K., Guan, Z.-Y., Yamagata, T., 2001. Impact of the Indian Ocean Dipole on the relationship between the Indian monsoon rainfall and ENSO. Geophysical Research Letters 28 (23), 4499–4502.
Banse, K., 1997. Irregular flow of Persian (Arabian) Gulf water to the Arabian Sea. Journal of Marine Research 55 (6), 1049–1067.
Banse, K., English, D.C., 1994. Seasonality of Coastal Zone Color Scanner phytoplankton pigment in the offshore oceans. Journal of Geophysical Research—Oceans 99 (C4), 7323–7345.
Banzon, V.F., Evans, R.E., Gordon, H.R., Chomko, R.M., 2004. SeaWiFS observations of the Arabian Sea southwest monsoon bloom for the year 2000. Deep-Sea Research Part II—Topical Studies in Oceanography 51 (1–3), 189–208.
Bergametti, G., Remoudaki, E., Losno, R., Steiner, E., Chatenet, B., 1992. Source, transport and deposition of atmospheric phosphorus over the northwestern Mediterranean. Journal of Atmospheric Chemistry 14 (1–4), 501–513.
Betzer, P.R., Carder, K.L., Duce, R.A., Merrill, J.T., Tindale, N.W., Uematau, M., Costello, D.K., Young, R.W., Feely, R.A., Breland, J.A., Bernstein, R.E., Greco, A.M., 1988. Long-range transport of giant mineral aerosol particles. Nature 336 (6199), 568–571.
Black, E., Slingo, J., Sperber, K.R., 2003. An observational study of the relationship between excessively strong short rains in coastal east Africa and Indian Ocean SST. Monthly Weather Review 131 (1), 74–94.
Brewer, P.G., Dyrssen, D., 1985. Chemical oceanography of the Persian Gulf. Progress in Oceanography 14 (1–4), 41–55.
Campbell, J.W., 1995. The lognormal-distribution as a model for biooptical variability in the sea. Journal of Geophysical Research—Oceans 100 (C7), 13237–13254.
Cannizzaro, J.P., Carder, K.L., 2006. Estimating chlorophyll *a* concentrations from remote-sensing reflectance in optically shallow waters. Remote Sensing of Environment 101 (1), 13–24.
Chase, Z., Paytan, A., Johnson, K.S., Street, J.H., Chen, Y., 2006. Input and cycling of iron in the Gulf of Aqaba, Red Sea. Global Biogeochemical Cycles 20 (3), GB3017.
Chen, Y., Mills, S., Street, J.H., Golan, D., Post, A.F., Jacobson, M., Paytan, A., 2007. Estimates of atmospheric dry deposition and associated input of nutrients to Gulf of Aqaba seawater. Journal of Geophysical Research—Atmospheres 112 (D04), D04309.
Chin, M., Rood, R.B., Lin, S.-J., Muller, J.-F., Thompson, A.M., 2000. Atmospheric sulfur cycle simulated in the global model GOCART: model description and global properties. Journal of Geophysical Research—Atmospheres 105 (D20), 24671–24687.
Claustre, H., Morel, A., Hooker, S.B., Babin, M., Antoine, D., Oubelkheir, K., Bricaud, A., Leblanc, K., Queguiner, B., Maritorena, S., 2002. Is desert dust making oligotrophic waters greener? Geophysical Research Letters 29 (10), 1469.
Coale, K.H., Johnson, K.S., Fitzwater, S.E., Gordon, R.M., Tanner, S., Chavez, F.P., Ferioli, L., Sakamoto, C., Rogers, P., Millero, F., Steinberg, P., Nightingale, P., Cooper, D., Cochlan, W.P., Landry, M.R., Constantinou, J., Rollwagen, G., Trasvina, A., Kudela, R.M., 1996. A massive phytoplankton bloom induced by an ecosystem-scale iron fertilization experiment in the equatorial Pacific Ocean. Nature 383 (6600), 495–501.
Cropp, R.A., Gabric, A.J., McTainsh, G.H., Braddock, R.D., Tindale, N.W., 2005. Coupling between ocean biota and atmospheric aerosols: dust, dimethylsulphide, or artifact? Global Biogeochemical Cycles 19 (4), CB4002.
Cullen, H.M., Kaplan, A., Arkin, P.A., Demenocal, P.B., 2002. Impact of the North Atlantic Oscillation on Middle Eastern climate and streamflow. Climatic Change 55 (3), 315–338.
deBaar, H.J.W., deJong, J.T.M., Bakker, D.C.E., Loscher, B.M., Veth, C., Bathmann, U., Smetacek, V., 1995. Importance of iron for plankton blooms and carbon dioxide drawdown in the Southern Ocean. Nature 373, 412–415.
Dubovik, O., Holben, B., Eck, T.F., Smirnov, A., Kaufman, Y.J., King, M., Tanre, D., Slutsker, I., 2002. Variability of absorption and optical properties of key aerosol types observed in worldwide locations. Journal of Atmospheric Sciences 59 (3), 590–608.
Duce, R.A., Tindale, N.W., 1991. Atmospheric transport of iron and its deposition in the ocean. Limnology and Oceanography 36 (8), 1715–1726.
Elshorbady, W., Azam, M.H., Taguchi, K., 2006. Hydrodynamic characterization and modeling of the Arabian Gulf. Journal of Waterway, Port, Coastal, and Ocean Engineering—ASCE 132 (1), 47–56.
Erickson, D.J., Hernandez, J.L., Ginoux, P., Gregg, W.W., McClain, C.R., Christian, J., 2003. Atmospheric iron delivery and surface ocean biological activity in the Southern Ocean and Patagonian region. Geophysical Research Letters 30 (12), 1609.
Evans, R.H., Gordon, H.R., 1994. Coastal zone color scanner "system calibration": a retrospective examination. Journal of Geophysical Research—Oceans 99 (C4), 7293–7307.
Foltz, G.R., McPhaden, M.J., 2008. Impact of Saharan dust on tropical North Atlantic SST. Journal of Climate 21 (19), 5048–5060.
Frouin, R., Franz, B. and Wang, M., 2001. Algorithm to estimate PAR from SeaWiFS data. Version 1.2 — Documentation.
Gordon, H.R., 1997. Atmospheric correction of ocean color imagery in the Earth Observing System era. Journal of Geophysical Research—Atmospheres 102 (D14), 17081–17106.
Gordon, H.R., Wang, M., 1994. Retrieval of water-leaving radiance and aerosol optical thickness over the oceans with SeaWiFS: a preliminary algorithm. Applied Optics 33 (3), 443–452.
Gordon, H.R., Brown, J.W., Brown, O.B., Evans, R.E., Clark, D.K., 1983. Nimbus 7 CZCS: reduction of its radiometric sensitivity with time. Applied Optics 22 (24), 3929–3931.
Goreau, T.J., McClannahan, T.R., Hayes, R., Strong, A.E., 2000. Conservation of coral reefs after the 1998 global bleaching event. Conservation Biology 14 (1), 5–15.
Guerzoni, S., Chester, R., Dulac, F., Herut, B., Loye-Pilot, M.-D., Measures, C., Migon, C., Molinaroli, E., Moulin, C., Rossini, P., Saydam, C., Soudine, A., Ziveri, P., 1999. The role of atmospheric deposition in the biogeochemistry of the Mediterranean Sea. Progress in Oceanography 44 (1–3), 147–190.
Herut, B., Collier, R., Krom, M.D., 2002. The role of dust in supplying nitrogen and phosphorus to the Southeast Mediterranean. Limnology and Oceanography 47 (3), 870–878.
Huang, H., Thomas, G.E., Grainger, R.G., 2009. Relationship between wind speed and aerosol optical depth over remote ocean. Atmospheric Chemistry and Physics Discussion 9 (6), 24511–24529.
Huffman, G.J., Adler, R.F., Morrissey, M.M., Bolvin, D.T., Curtis, S., Joyce, R., McGavock, B., Susskind, J., 2001. Global precipitation at one-degree daily resolution from multisatellite observations. Journal of Hydrometeorology 2 (1), 36–50.
Husar, R.B., Prospero, J.M., Stowe, L.L., 1997. Characterization of tropospheric aerosols over the oceans with the NOAA advanced very high resolution radiometer optical thickness operational product. Journal of Geophysical Research—Atmospheres 102 (D14), 16889–16909.
Ignatov, A.M., 2002. Sensitivity and information content of aerosol retrievals from the Advanced Very High Resolution Radiometer: radiometric factors. Applied Optics 41 (6), 991–1011.
Ignatov, A.M., Minnis, P., Miller, W.F., Wielicki, B.A., Remer, L.A., 2006. Consistency of global MODIS aerosol optical depths over ocean on Terra and Aqua CERES SSF data sets. Journal of Geophysical Research—Atmospheres 111 (D14), D14202.
Jickells, T.D., An, Z.S., Andersen, K.K., Baker, A.R., Bergametti, G., Brooks, N., Cao, J.J., Boyd, P.W., Duce, R.A., Hunter, K.A., Kawahata, H., Kubilay, N., laRoche, J., Liss, P.S., Mahowald, N., Prospero, J.M., Ridgwell, A.J., Tegen, I., Torres, R., 2005. Global iron connections between desert dust, ocean biogeochemistry, and climate. Science 308 (5718), 67–71.
John, V.C., 1992. Circulation and mixing processes and their effect on pollution distribution in the western Arabian Gulf. Applied Ocean Research 14 (1), 59–64.
Johns, W.E., Yao, F., Olson, D.B., Josey, S.A., Grist, J.P., Smeed, D.A., 2003. Observations of seasonal exchange through the Straits of Hormuz and the inferred heat and freshwater budgets of the Persian Gulf. Journal of Geophysical Research—Oceans 108 (C12), 3391.
Kahru, M., Mitchell, B.G., 2008. Ocean color reveal increased blooms in various parts of the world. EOS 89 (18), 170.
Kalnay, E., Kanamitsu, M., Kistler, R., Collins, W., Deaven, D., Gandin, L., Iredell, M., Saha, S., White, G., Woollen, J., Zhu, Y., Chelliah, M., Ebisuzaki, W., Higgins, W., Janowiak, J., Mo, K.C., Ropelewski, C.F., Wang, J., Leetmaa, A., Reynolds, R., Jenne, R., Joseph, D., 1996. The NCEP/NCAR 40-year reanalysis project. Bulletin of the American Meteorological Society 77 (3), 437–471.

Author's personal copy

Kilpatrick, K.A., Podesta, G.P., Evans, R., 2001. Overview of the NOAA/NASA advanced very high resolution radiometer Pathfinder algorithm for sea surface temperature and associated matchup database. Journal of Geophysical Research—Oceans 106 (C5), 9179–9197.

Kinne, S., Lohmann, U., Feichter, J., Schulz, M., Timmreck, C., Ghan, S., Easter, R., Chin, M., Ginoux, P., Takemura, T., Tegen, I., Koch, D., Herzog, M., Penner, J., Pitari, G., Holben, B., Eck, T., Smirnov, A., Dubovik, O., Slutsker, I., Tanre, D., Torres, O., Mishchenko, M., Geogdzhayev, I.V., Chu, D.A., Kaufman, Y.J., 2003. Monthly averages of aerosol properties: a global comparison among models, satellite data, and AERONET ground data. Journal of Geophysical Research—Atmospheres 108 (D20), 4634.

Koch, D., Jacob, D., Tegen, I., Rind, D., Chin, M., 1999. Tropospheric sulfur simulation and sulfate direct radiative forcing in the Goddard Institute for Space Studies general circulation model. Journal of Geophysical Research—Atmospheres 104 (D19), 23799–23822.

Lehahn, Y., Koren, I., Boss, E.S., Ben-Ami, Y., Altaratz, O., 2010. Estimating the maritime component of aerosol optical depth and its dependency on surface wind speed using MODIS and QuikSCAT data. Atmospheric Chemistry and Physics Discussion 10 (1), 1983–2003.

Levy, M., Shankar, D., Andre, J.M., Shenoi, S.S.C., Durand, F., Montegut, C.d.B., 2007. Basin-wide seasonal evolution of the Indian Ocean's phytoplankton blooms. Journal of Geophysical Research—Oceans 112 (C12), C12014.

Levy, R.C., Leptoukh, G.G., Kahn, R., Zubko, V., Gopalan, A., Remer, L.A., 2009. A critical look at deriving monthly aerosol optical depth from satellite data. IEEE Transactions on Geoscience and Remote Sensing 47 (8), 2942–2956.

Li, Z., Zhao, X., Kahn, R., Mishchenko, M., Remer, L., Lee, K.H., Wang, M., Laszlo, I., Nakajima, T., Maring, H., 2009. Uncertainties in satellite remote sensing of aerosols and impact on monitoring its long-term trend: a review and perspective. Annales Geophysicae 27 (7), 2755–2770.

Longhurst, A.R., 1995. Seasonal cycles of pelagic production and consumption. Progress in Oceanography 36 (2), 77–167.

Mackey, K.R.M., Labiosa, R.G., Calhoun, M., Street, J.H., Post, A.F., Paytan, A., 2007. Phosphorus availability, phytoplankton community dynamics, and taxon-specific phosphorus status in the Gulf of Aqaba, Red Sea. Limnology and Oceanography 52 (2), 873–885.

Mahowald, N.M., Baker, A.R., Bergametti, G., Brooks, N., Duce, R.A., Jickells, T.D., Kubilay, N., Prospero, J.M., Tegen, I., 2005. Atmospheric global dust cycle and iron inputs to the ocean. Global Biogeochemical Cycles 19 (4), CB4025.

Mallet, M., Chami, M., Gentili, B., Sempere, R., Dubuisson, P., 2009. Impact of sea-surface dust radiative forcing on the oceanic primary production: a 1D modeling approach applied to the West African coastal waters. Geophysical Research Letters 36, L15828.

Marcella, M.P., Eltahir, E.A.B., 2008. The hydroclimatology of Kuwait: explaining the variability of rainfall at seasonal and interannual time scales. Journal of Hydrometeorology 9 (5), 1095–1105.

Maritorena, S., Morel, A.Y., Gentili, B., 1994. Diffuse reflectance of oceanic shallow waters: influence of water depth and bottom albedo. Limnology and Oceanography 39 (7), 1689–1703.

Markaki, Z., Oikonomou, K., Kocak, M., Kouvarakis, G., Chaniotaki, A., Kubilay, N., Mihalopoulos, N., 2003. Atmospheric deposition of inorganic phosphorus in the Levantine Basin, eastern Mediterranean: spatial and temporal variability and its role in seawater productivity. Limnology and Oceanography 48 (4), 1557–1568.

Martin, J.-M., Elbaz-Poulichet, F., Guieu, C., Loye-Pilot, M.-D., Han, G., 1989. River versus atmospheric input of material to the Mediterranean Sea: an overview. Marine Chemistry 28 (1–3), 159–182.

Martin, J.H., Gordon, R.M., Fitzwater, S.E., 1991. The case for iron. Limnology and Oceanography 36 (8), 1793–1802.

Martin, J.H., Coale, K.H., Johnson, K.S., Fitzwater, S.E., Gordon, R.M., Tanner, S.J., Hunter, C.N., Elrod, V.A., Nowicki, J.L., Coley, T.L., Barber, R.T., Lindley, S., Watson, A.J., Van Scoy, K., Law, C.S., Liddlcoat, M.I., Ling, R., Stanton, T., Stockel, J., Collins, C., Anderson, A., Bidigare, R.R., Ondrusek, M., Latasa, M., Millero, F.J., Lee, K., Yao, W., Zhang, J.Z., Friederich, G.E., Sakamoto, C., Chavez, F.P., Buck, K.R., Kolber, Z., Greene, R., Falkowski, P.G., Chisholm, S.W., Hoge, F.E., Swift, R., Yungel, J., Turner, S., Nightingale, P., Hatton, A., Liss, P., Tindale, N.W., 1994. Testing the iron hypothesis in ecosystems of the equatorial Pacific Ocean. Nature 371 (6493), 123–129.

McPhaden, M.J., 1999. Genesis and evolution of the 1997–98 El Niño. Science 283 (5404), 950–954.

Meskhidze, N., Chameides, W.L., Nenes, A., 2005. Dust and pollution: a recipe for enhanced ocean fertilization? Journal of Geophysical Research—Atmospheres 110 (D3), D03301.

Morel, A., Prieur, L., 1977. Analysis of variations in ocean color. Limnology and Oceanography 22 (4), 709–722.

Moulin, C., Gordon, H.R., Chomko, R.M., Banzon, V.F., Evans, R.H., 2001. Atmospheric correction of ocean color imagery through thick layers of Saharan dust. Geophysical Research Letters 28 (1), 5–8.

Mulcahy, J.P., O'Dowd, C.D., Jennings, S.G., Ceburnis, D., 2008. Significant enhancement of aerosol optical depth in marine air under high wind conditions. Geophysical Research Letters 35 (16), L16810.

Muller-Karger, F.E., Hu, C., Andrefouet, S., Varela, R., Thunell, R.C., 2005. The color of the coastal ocean and applications in the solution of research and management problems. In: Miller, R.L., Del Castillo, C.E., McKee, B.A. (Eds.), Remote Sensing of Coastal Aquatic Environments. Springer, Dordrecht, pp. 101–127.

Myhre, G., Stordal, F., Johnsrud, M., Diner, D.J., Geogdzhayev, I.V., Haywood, J.M., Holbein, B.N., Holzer-Popp, T., Ignatov, A.M., Kahn, R.A., Kaufman, Y.J., Loeb, N., Martonchik, J.V., Mishchenko, M.I., Nalli, N.R., Remer, L.A., Schroedter-Homscheidt, M., Tanre, D., Torres, O., Wang, M., 2005. Intercomparison of satellite retrieved aerosol optical depth over ocean during the period September 1997 to December 2000. Atmospheric Chemistry and Physics 5 (6), 1697–1719.

Neuer, S., Torres-Padron, M.E., Gelado-Caballero, M.D., Rueda, M.J., Hernandez-Brito, J., Davenport, R., Wefer, G., 2004. Dust deposition pulses to the eastern subtropical North Atlantic gyre: does ocean's biogeochemistry respond? Global Biogeochemical Cycles 18 (4), GB4020.

Nezlin, N.P., Stein, E.D., 2005. Spatial and temporal patterns of remotely-sensed and field-measured rainfall in southern California. Remote Sensing of Environment 96 (2), 228–245.

O'Neil, N.T., Ignatov, A.M., Holbein, B.N., Eck, T.F., 2000. The lognormal distribution as a reference for reporting aerosol optical depth statistics; empirical tests using multi-year, multi-site AERONET sunphotometer data. Geophysical Research Letters 27 (20), 3333–3336.

O'Reilly, J.E., Maritorena, S., Mitchell, B.G., Siegel, D.A., Carder, K.L., Garver, S.A., Kahru, M., McClain, C., 1998. Ocean color chlorophyll algorithms for SeaWiFS. Journal of Geophysical Research—Oceans 103 (C11), 24937–24953.

Paerl, H.W., 1997. Coastal eutrophication and harmful algal blooms: importance of atmospheric deposition and groundwater as "new" nitrogen and other nutrient sources. Limnology and Oceanography 42 (5, part 2), 1154–1165.

Patra, P.K., Kumar, M.D., Mahowald, N., Sarma, V.V.S.S., 2007. Atmospheric deposition and surface stratification as controls of contrasting chlorophyll abundance in the North Indian Ocean. Journal of Geophysical Research—Oceans 112 (C5), C05029.

Paytan, A., Mackey, K.R.M., Chen, Y., Lima, I.D., Doney, S.C., Mahowald, N., Labiosa, R.G., Post, A.F, 2009. Toxicity of atmospheric aerosols on marine phytoplankton. Proceedings of the National Academy of Sciences of the United States of America 106 (12), 4601–4605.

Pease, P.P., Tchakerian, V.P., Tindale, N.W., 1998. Aerosols over the Arabian Sea: geochemistry and source areas for aeolian desert dust. Journal of Arid Environments 39 (3), 477–496.

Prasad, T.G., Ikeda, M., Kumar, S.P., 2001. Seasonal spreading of the Persian Gulf Water mass in the Arabian Sea. Journal of Geophysical Research—Oceans 106 (C8), 17059–17071.

Praveen, P.S., Rao, P.S.P., Safai, P.D., Devara, P.C.S., Chate, D.M., Ali, K., Momin, G.A., 2007. Study of aerosol transport through precipitation chemistry over Arabian Sea during winter and summer monsoons. Atmospheric Environment 41 (4), 825–836.

Privett, D.W., 1959. Monthly charts of evaporation from the Indian Ocean (including the Red Sea and the Persian Gulf). Quarterly Journal Royal Meteorological Society 85 (366), 424–428.

Ransibrahmanakul, V., Stumpf, R.P., 2006. Correcting ocean colour reflectance for absorbing aerosols. International Journal of Remote Sensing 27 (9), 1759–1774.

Remer, L.A., Kaufman, Y.J., Tanre, D., Mattoo, S., Chu, D.A., Martins, J.V., Li, R.R., Ichoku, C., Levy, R.C., Kleidman, R.G., Eck, T.F., Vermote, E.F., Holben, B.N., 2005. The MODIS aerosol algorithm, products, and validation. Journal of Atmospheric Sciences 62 (4), 947–973.

Reynolds, R.M., 1993. Physical oceanography of the Gulf, Strait of Hormuz, and the Gulf of Oman—results from the Mt. Mitchell expedition. Marine Pollution Bulletin 27, 35–59.

Riegl, B., 2002. Effects of the 1996 and 1998 positive sea-surface temperature anomalies on corals, coral diseases and fish in the Arabian Gulf (Dubai, UAE). Marine Biology 140 (1), 29–40.

Rodionov, S.N., 1994. Global and regional climate interaction: the Caspian Sea experience. Water Science and Technology Library. Kluwer Academic Publishers, Dordrecht. 241 pp.

ROPME, 2009. First Meeting of the Regional Task Force on Harmful Algal Blooms (HABs) and Related Marine Mortality in the ROPME Sea Area, ROPME, 26–28 January 2009. ROPME, Kuwait.

Sadrinasab, M., Kampf, J., 2004. Three-dimensional flushing times of the Persian Gulf. Geophysical Research Letters 31 (24), L24301.

Safar, M.I., 1985. Dust and Dust Storms in Kuwait. Directorate of Civil Aviation Meteorological Department, State of Kuwait.

Saji, N.H., Goswami, B.N., Vinayachandran, P.N., Yamagata, T., 1999. A dipole mode in the tropical Indian Ocean. Nature 401 (6751), 360–363.

Sheppard, C.R.C., 1993. Physical environment of the Gulf relevant to marine pollution: an overview. Marine Pollution Bulletin 27, 3–8.

Siegel, D.A., Wang, M., Maritorena, S., Robinson, W., 2000. Atmospheric correction of satellite ocean color imagery: the black pixel assumption. Applied Optics 39 (21), 3582–3591.

Singh, R.P., Prasad, A.K., Kayetha, V.K., Kafatos, M., 2008. Enhancement of oceanic parameters associated with dust storms using satellite data. Journal of Geophysical Research—Oceans 113 (C11), C11008.

Subba Rao, D.V., Al-Yamani, F., 1998. Phytoplankton ecology in the waters between Shatt Al-Arab and Straits of Hormuz, Arabian Gulf: a review. Plankton Biology and Ecology 45 (2), 106–116.

Subba Rao, D.V., Al-Yamani, F., 1999a. Analysis of the relationship between phytoplankton biomass and the euphotic layer off Kuwait, Arabian Gulf. Indian Journal of Marine Sciences 28 (4), 416–423.

Subba Rao, D.V., Al-Yamani, F., 1999b. Eolian dust affects phytoplankton in the waters off Kuwait, the Arabian Gulf. Naturwissenschaften 86 (11), 525–529.

Sultan, S.A.R., Elghribi, N.M., 1996. Temperature inversion in the Arabian Gulf and the Gulf of Oman. Continental Shelf Research 16 (12), 1521–1544.

Sunda, W.G., Huntsman, S.A., 1997. Interrelated influence of iron, light and cell size on marine phytoplankton growth. Nature 390 (6658), 389–392.

Swift, S.A., Bower, A.S., 2003. Formation and circulation of dense water in the Persian/Arabian Gulf. Journal of Geophysical Research—Oceans 108 (C1), 3004.

Tanre, D., Kaufman, Y.J., Herman, M., Mattoo, S., 1997. Remote sensing of aerosol properties over oceans using the MODIS/EOS spectral radiances. Journal of Geophysical Research—Atmospheres 102 (D14), 16971–16988.

Tegen, I., Koch, D., Lacis, A.A., Sato, M., 2000. Trends in tropospheric aerosol loads and corresponding impact on direct radiative forcing between 1950 and 1990: a model study. Journal of Geophysical Research—Atmospheres 105 (D22), 26971–26989.

Author's personal copy

Torres, O., Bhartia, P.K., Herman, J.R., Ahmad, Z., Gleason, J., 1998. Derivation of aerosol properties from satellite measurements of backscattered ultraviolet radiation: theoretical basis. Journal of Geophysical Research—Atmospheres 103 (D14), 17099–17110.

Volpe, G., Banzon, V.F., Evans, R.H., Santoleri, R., Mariano, A.J., Sciarra, R., 2009. Satellite observations of the impact of dust in a low-nutrient, low-chlorophyll region: fertilization or artifact? Global Biogeochemical Cycles 23, BG3007.

Walsh, J.J., Jolliff, J.K., Darrow, B.P., Lenes, J.M., Milroy, S.P., Remsen, A., Dieterle, D.A., Carder, K.L., Chen, F.R., Vargo, G.A., Weisberg, R.H., Fanning, K.A., Muller-Karger, F.E., Shinn, E., Steidinger, K.A., Heil, C.A., Tomas, C.R., Prospero, J.S., Lee, T.N., Kirkpatrick, G.J., Whitledge, T.E., Stockwell, D.A., Villareal, T.A., Jochens, A.E., Bontempi, P.S., 2006. Red tides in the Gulf of Mexico: where, when, and why? Journal of Geophysical Research—Oceans 111 (C11), C11003.

Walton, C.C., 1988. Nonlinear multichannel algorithms for estimating sea surface temperature with AVHRR satellite data. Journal of Applied Meteorology 27 (2), 115–124.

Wiggert, J.D., Murtugudde, R.D., 2007. The sensitivity of the southwest monsoon phytoplankton bloom to variations in aeolian iron deposition over the Arabian Sea. Journal of Geophysical Research—Oceans 112 (C05), C05005.

Wynne, T.T., Stumpf, R.P., Richardson, A.G., 2006. Discerning resuspended chlorophyll concentrations from ocean color satellite imagery. Continental Shelf Research 26 (20), 2583–2597.